DOI: 10.24352/UB.OVGU-2017-084 TECHNISCHE MECHANIK, 37, 1, (2017), 82 – 106
submitted: March 21, 2017

Generalized Collocation Method using Stiffness Matrices in the Context of the Theory of Linear Viscoelasticity (GUSTL)

M. A. Kraus, M. Niederwald

*This paper presents a methodology called GUSTL (**G**eneralized collocation method **u**sing **S**tiffness matrices in the context of the **T**heory of **L**inear viscoelasticity), which is designed to efficiently estimate the parameters of a Prony-series representation using measured data of the complex modulus $\mathbf{E}^*$ of a viscoelastic material obtained via a dynamic mechanical thermal analysis (DMA or DMTA). The methodology is based on the idea of solving an inverse problem, which is established as a physically motivated system of linear equations. The "stiffness matrix" of this problem is derived out of the interdepencies of the single elements of the Generalized–Maxwell–Elements. Further extensions of the method to the incorporation of the time–temperature–superposition (TTS) principle as well as uncertainty quantification tasks are also highlighted. The whole methodology is validated against sample data from an epoxy–coated carbon reinforcement grid for concrete structures and from a PVB–interlayer material for laminated safety glass.*

1 Motivation

In modern civil engineering applications many materials, such as coated carbon reinforcement grids for concrete structures or PVB-interlayers for safety glass, are polymer based. Usually these materials show strong strain-rate (viscoelastic) and temperature dependent behaviour. In literature different mathematical representations (such as the hereditary integral representation or the formulation via differential equations (Flügge (1975)) and exist. A very common representation is using the Prony–series approach, which is implemented in many FEA software to incorporate linear viscoelastic material behaviour. The thermomechanical properties of polymers are often characterised by the glass–transition temperature T_g, which defines the temperature at which polymers change their state from glassy (solid) to rubbery. The glass–transition temperature is very dependent on the chemistry of the polymer (for the epoxy adhesive investigated in this paper it lies between $60°C$ to $130°C$ and for a standard PVB–interlayer material for structural glazing it lies between $20°C$ to $70°C$).

The experimental determination of the Prony–series and its parameters can either be conducted via data from relaxation or retardation experiments in the time domain or from data taken under a steady state oscillation in the frequency domain, which is known as the dynamic mechanical thermal analysis (DMA or DMTA). As the experiments in the time domain are very time consuming, usually the DMA is the preferred choice to obtain the viscoelastic material behaviour in a very narrow time span.

While the mathematical framework for calculation and simulating the material response given an applied excitation and the corresponding Prony–series is a simple task, the inverse problem of obtaining the Prony–series representation of a viscoelastic modulus from rate dependent data is complex. Usually the number of conducted tests is limited by economical and / or organizational constraints. Hence the data source for identification of the system behaviour as well as further statistical calculations such as parameter estimation is sparse. This data–sparsity introduces uncertainty in the whole estimation process. Different authors dealt with the parameter identification problem in the past. For fitting experimental data in the time domain (Tschoegl (1989), Tschoegl and Emri (1993); Emri and Tschoegl (1994, 1995)) and many others provided methods and proofed their success. Also for fitting experimental data in the frequency domain different methods are available, c.f. (Tschoegl (1989), Tschoegl and Emri (1993); Emri and Tschoegl (1994, 1995), Mead (1994), Elster et al. (1992); Honerkamp and Weese (1989)) etc.

With this work we motivate a fast nonnegative least-squares solution of the model parameter estimation procedure

for a Prony–series representation of the linear-viscoelastic material behaviour when DMA data are given. Via two examples from state–of–the–art research in structural engineering we show the capabilities of GUSTL. In the final section we motivate further extensions of the presented method GUSTL, which will take into consideration a Bayesian reformulation of the parameter estimation problem as well as extensions the time-temperature-superposition principle.

2 Basic Definitions and Concepts

2.1 Dynamic Mechanical Analysis - Equipment, Experiment and Theory

The dynamic mechanical analysis (DMA) or dynamic mechanical thermal analysis (DMTA) is a state–of–the–art testing method for viscoelastic materials, in which the material properties can be determined with a steady state oscillation. This approach is usually referred to as when the material properties are determined and expressed in terms of temperature as well as frequency. At the University of German Armed Forces Munich the DMTA can be conducted via a machine "EPLEXOR 2000N" from the manufacturer GABO.
The principle of DMA is to apply a sinusoidal stress or strain to the specimen and to measure the material response. From this, it is possible to determine the stiffness of the material and also its viscosity from the phase lag δ between the oscillating stress or strain and the material response, as illustrated in Fig. 1a.

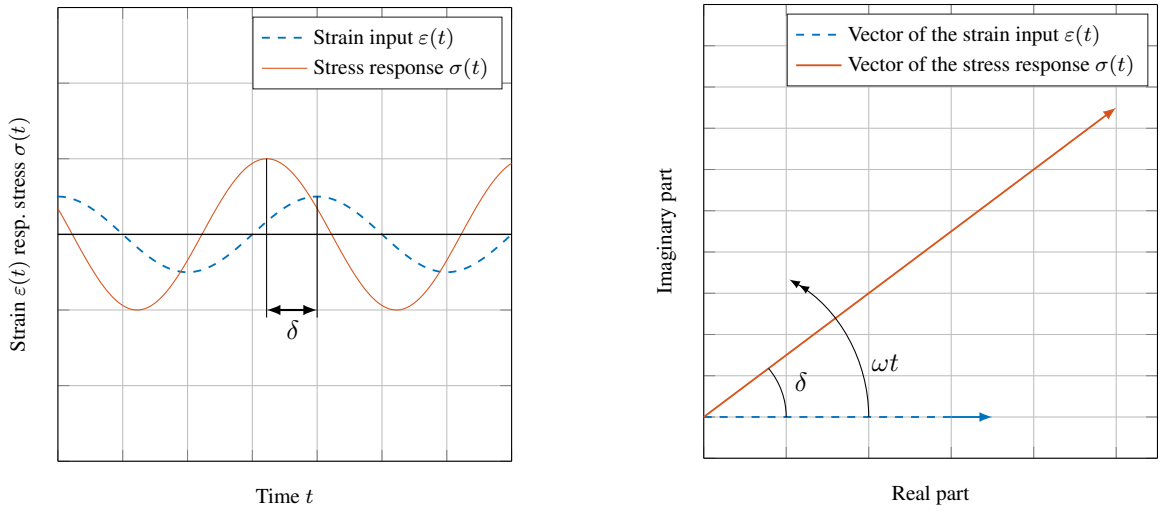

(a) Phase lag between strain input and stress response

(b) Strain input and stress response in the complex plane

Figure 1. Principle of dynamic mechanical analysis (Menard (1999), Roylance (2001)), picture taken from Kraus et al. (2016)

The DMA–tests are usually conducted by application of forced vibrations while sweeping across different frequencies. The measurements are repeated for different constant temperatures in order to investigate the temperature dependency of viscoelastic material behaviour.

2.2 Theory of Linear Viscoelasticity and the Generalized Maxwell Element in the Time and Frequency Domain

2.2.1 Theory of Linear Viscoelasticity

The Generalized Maxwell model (see Fig. 2) possesses K Maxwell models (one spring and one viscous damper in series) and one isolated spring so it is a composition of $K + 1$ constituent elements (c.f. Tschoegl (1989)).

The model is described by Eq. 1

$$E(t) = E + \sum_{k=1}^{K} \hat{E}_k \, e^{-\frac{t}{\tau_k}} \tag{1}$$

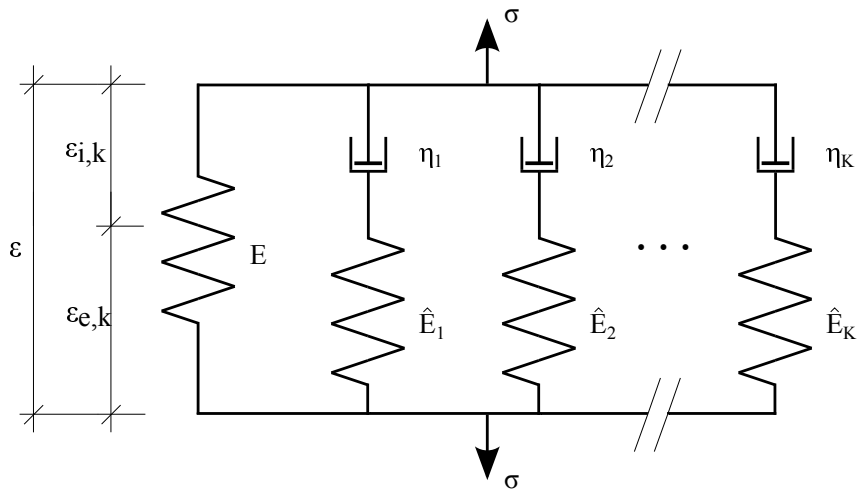

Figure 2. Generalized Maxwell model (Flügge (1975)), picture taken from Kraus et al. (2016)

Eq. 1 is usually referred to as the Prony–series. This function can also be given in dimensionless form:

$$r(t) = \frac{E(t)}{E_0} = \frac{E}{E_0} + \sum_{k=1}^{K} \frac{\hat{E}_k}{E_0}\, e^{-\frac{t}{\tau_k}} = r + \sum_{k=1}^{K} r_k\, e^{-\frac{t}{\tau_k}} = 1 - \sum_{k=1}^{K} r_k \left(1 - e^{-\frac{t}{\tau_k}}\right) \tag{2}$$

with $E + \sum_k^K \widehat{E}_k = E_0$

A closer look at the Prony-series allows a new interpretation in terms of the Prony-series being an inner product (or scalar product):

$$E(t) = \begin{pmatrix} E \\ \hat{E}_1 \\ \vdots \\ \hat{E}_K \end{pmatrix}^T \cdot \begin{pmatrix} 1 \\ exp(-\frac{t}{\tau_1}) \\ \vdots \\ exp(-\frac{t}{\tau_K}) \end{pmatrix} = \begin{pmatrix} E & \hat{E}_1 & \dots & \hat{E}_K \end{pmatrix} \cdot \begin{pmatrix} 1 \\ exp(-\frac{t}{\tau_1}) \\ \vdots \\ exp(-\frac{t}{\tau_K}) \end{pmatrix} = < \underline{\mathbf{G}}, \underline{\mathbf{B}} > \tag{3}$$

where the $\hat{E}_k$ are the coordinates (summarized in the coordinate vector $\underline{\mathbf{G}}$) and the $\underline{\mathbf{b}}_k = e^{-\frac{t}{\tau_k}}$ are the basis functions (summarized in the common basis vector $\underline{\mathbf{B}}$).

In the context of the theory of linear viscoelasticity the validity of the BOLTZMANN superposition principle (Bergström (2015)) (which is sometimes referred to as DUHAMEL'S integral (Clough and Penzien (1975))) is assumed. This simply means, that the material response due to the sum of two different excitations can be superimposed from the individual material responses due to each excitation.

2.2.2 The generalized Maxwell Element in the Time and Frequency Domain

Taking the Fourier transform of Eq. 3, the result to obtain is:

$$\mathbf{E}^*(\omega) = E + \sum_{k=1}^{K} \hat{E}_k \frac{\omega^2\, {\tau_k}^2}{1 + \omega^2\, {\tau_k}^2} + i \sum_{k=1}^{K} \hat{E}_k \frac{\omega\, \tau_k}{1 + \omega^2\, {\tau_k}^2} \tag{4}$$

Where the real part ($\Re(\mathbf{E}^*) = E'$) of Eq. 4 is called the storage modulus and the imaginary part ($\Im(\mathbf{E}^*) = E''$) is called loss modulus as described above.

Analogously as it was done in Sec. 2.2.1, the storage and loss modulus can be formulated as an inner product. For the storage and loss modulus this reads:

$$E'(\omega) = \begin{pmatrix} E \\ \hat{E}_1 \\ \vdots \\ \hat{E}_K \end{pmatrix}^T \cdot \begin{pmatrix} 1 \\ \frac{\omega^2 \tau_1{}^2}{1+\omega^2 \tau_1{}^2} \\ \vdots \\ \frac{\omega^2 \tau_K{}^2}{1+\omega^2 \tau_K{}^2} \end{pmatrix} = \begin{pmatrix} E & \hat{E}_1 & \dots & \hat{E}_K \end{pmatrix} \begin{pmatrix} 1 \\ \frac{\omega^2 \tau_1{}^2}{1+\omega^2 \tau_1{}^2} \\ \vdots \\ \frac{\omega^2 \tau_K{}^2}{1+\omega^2 \tau_K{}^2} \end{pmatrix} =< \underline{\mathbf{G}}, \underline{\mathbf{B}}' > \tag{5}$$

$$E''(\omega) = \begin{pmatrix} E \\ \hat{E}_1 \\ \vdots \\ \hat{E}_K \end{pmatrix}^T \cdot \begin{pmatrix} 0 \\ \frac{\omega \tau_1}{1+\omega^2 \tau_1{}^2} \\ \vdots \\ \frac{\omega \tau_K}{1+\omega^2 \tau_K{}^2} \end{pmatrix} = \begin{pmatrix} E & \hat{E}_1 & \dots & \hat{E}_K \end{pmatrix} \begin{pmatrix} 0 \\ \frac{\omega \tau_1}{1+\omega^2 \tau_1{}^2} \\ \vdots \\ \frac{\omega \tau_K}{1+\omega^2 \tau_K{}^2} \end{pmatrix} =< \underline{\mathbf{G}}, \underline{\mathbf{B}}'' > \tag{6}$$

where the $\hat{E}_k$ are the coordinates (summarized in the coordinate vector $\underline{\mathbf{G}}$) and the $\underline{\mathbf{b}}'_k = \frac{\omega^2 \tau_K^2}{1+\omega^2 \tau_K{}^2}$ (summarized in the storage basis vector $\underline{\mathbf{B}}'$) respectively $\underline{\mathbf{b}}''_k = \frac{\omega \tau_K}{1+\omega^2 \tau_k{}^2}$ (summarized in the loss basis vector $\underline{\mathbf{B}}''$) are the basis functions. This inner product representation will be used in sec. 4 to define a regression problem.

A special focus shall now be laid on the "influence lengths" of the basis functions of the storage and loss moduli as this is the core for the later deduction of the stiffness matrix of the GUSTL methodology. The influence length describes the numbers of frequency decades over which a single Maxwell element influences the behaviour of storage and loss modulus.

Without loss of generality lets consider the following 5 Maxwell elements with parameters $\theta = [E; \hat{E}_1; \tau_1] = [0; k; 10^{-5-k}]$ with $k \in \{1, ..., 5\}$. The storage and loss moduli for each of these 5 Maxwell elements are given in the following two figures:

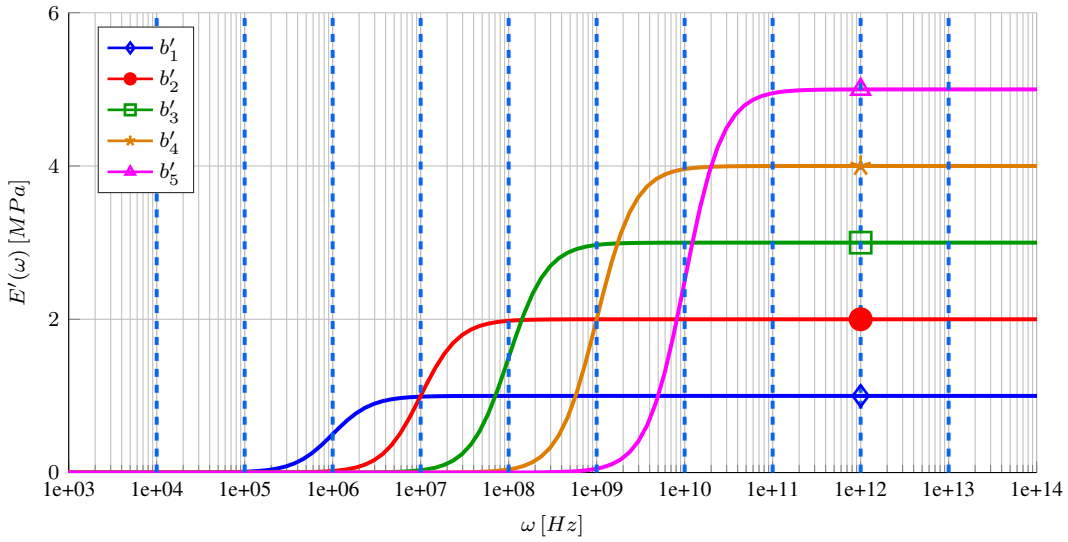

Figure 3. Influence length of the basis functions of the storage modulus $\underline{\mathbf{b}}'_k$

It is important to note the following things with respect to the real and imaginary part of a complex modulus:

- the storage modulus $E'(\omega)$ is a non–decreasing function of the frequency over the whole ω domain,
- if the frequency ω reaches $\frac{1}{\tau_k}$, the contribution of the $k-$th Maxwell element to the storage and loss modulus is $0.5 \cdot E_k$.

The first statement can be shown by taking the first derivative of E' w.r.t. ω and evaluating it over the whole ω domain. The second statement for the storage modulus E' can be proven by evaluating $E'(\omega = \frac{1}{\tau_k})$ as well as the loss modulus $E''(\omega = \frac{1}{\tau_k})$.

At this point only a qualitative study of the interdependence of the single Maxwell elements between each other and on the whole Prony–series is done by using figures 3 and 4. A further quantification is done in section 4.

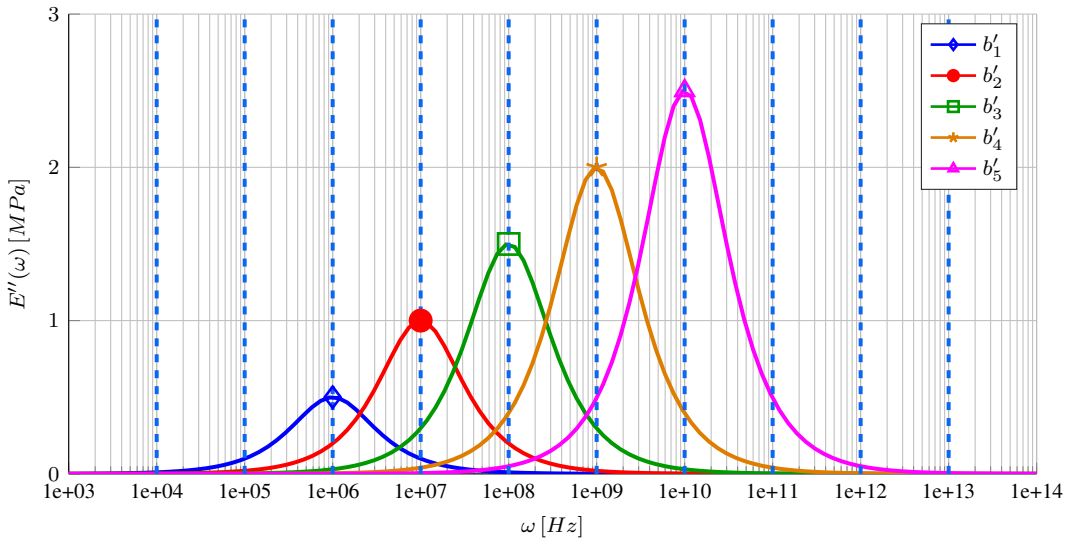

Figure 4. Influence length of the basis functions of the loss modulus $\underline{\mathbf{b}}''_k$

For the storage modulus the main behaviour of a single Maxwell element happens within two decades. The contribution of a single Maxwell element is zero until one decade before its characteristic relaxation frequency $\widetilde{\omega}_k = \frac{1}{\tau_k}$ and constantly E_k one decade after its characteristic relaxation frequency $\widetilde{\omega}_k$ (the single Maxwell element is therefore bandlimited in E_k over the whole ω domain), c.f. Fig. 3. This will later explain the lower–triangular structure of the "stiffness" matrix resulting from the Storage modulus.

For the loss modulus the main behaviour of a single Maxwell element happens within four decades, when a numerical precision of $0{,}2{\cdot}10^{-2}$ is considered. The contribution of a single Maxwell element is almost zero (in terms of numerical precision) until two decades before and two decades after its characteristic relaxation frequency $\widetilde{\omega}_k$, c.f. Fig. 3. The single Maxwell element is therefore (numerically) bandlimited in ω. This later explains the band–structure of the "stiffness" matrix resulting from the loss modulus.

Based on this knowledge, in section 4 the "stiffness" matrices for the storage modulus as well as the loss modulus are deduced and combined with the measurement data to form a system of linear equations, which is solved using a non–negative least–squares approach.

2.3 Time Temperature Superposition Principle and the "Master Curving" Process

Viscoelastic material properties of polymers strongly depend on the temperature. Typically, an increase in temperature at an equal strain rate causes a decreasing stiffness and vice versa. Temperature changes mainly influence the relaxation behaviour (Schwarzl (1990)), which leads to changing relaxation times (this is referred to as thermorheological simplicity). With increasing temperature relaxation times decrease and vice versa. Typically, a relaxation experiment takes longer in order to capture the stiffness behaviour over the time with satisfying precision, to obtain similar curves for other temperatures would require a large number of tests and would be a very time consuming procedure. Instead, a time–temperature–superposition (abbr. TTSP) procedure can be used to extract a so called "master curve" by performing short–term tests at different temperatures and shifting the measured curves on the time scale as illustrated in Fig. 5. The master curve can then be further shifted to determine the material response for any temperature of interest based on the given data set.

Mathematically, the TTSP can be deduced from an expression of the viscoelastic modulus as a Prony–series as given by Eq. 1, where the relaxation times $\tau_{j,Tref}$ at the reference temperature T_{ref} can be related to those at any other temperature T via the shift factor a_T:

$$\tau_j(T) = \tau_{j,Tref} \cdot a_T(T) \tag{7}$$

The modulus at another temperature T can thus be expressed in the time domain:

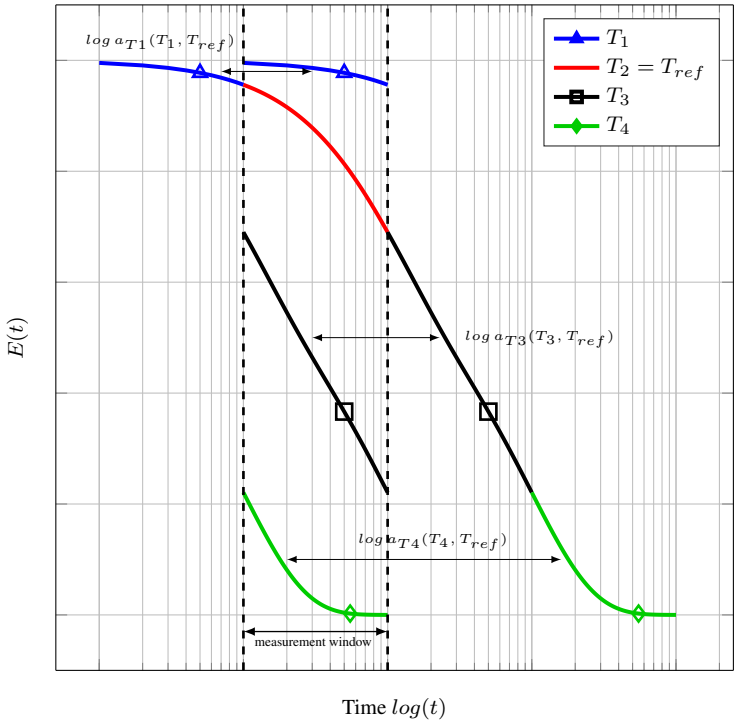

Figure 5. Time temperature superposition principle (TTSP) (Schwarzl (1990)), picture taken from Kraus et al. (2016)

$$E(t) = E + \sum_{k=1}^{K} \hat{E}_k \, e^{-\frac{t}{a_T(T)\,\tau_{k,Tref}}} = E + \sum_{k=1}^{K} \hat{E}_k \, e^{-\frac{\xi}{\tau_{k,Tref}}} \tag{8}$$

with $\xi = \frac{t}{a_T(T)}$ being called reduced time. In the frequency domain an analogous formula with the reduced frequency $\zeta = \omega \cdot a_T(T)$ can be found:

$$E(\omega) = E + \sum_{k=1}^{K} \hat{E}_k \, \frac{\zeta^2 \, (\tau_{k,Tref})^2}{1 + \zeta^2 \, (\tau_{k,Tref})^2} + i \sum_{k=1}^{K} \hat{E}_k \, \frac{\zeta \, \tau_{k,Tref}}{1 + \zeta^2 \, (\tau_{k,Tref})^2} \tag{9}$$

Although the principle of time–temperature–superposition seems to be rather simple performing it on actual measurement data in a numerical framework is a difficult task because of measurement errors influencing the shift process. Within this work a MATLAB code was developed in which the storage modulus curves for each measured temperature in the frequency domain are fitted with a cubic spline function. The curve–fit has the constrains that it runs through the first and the last data point. In the next step the overlapping on the storage modulus axes of two consecutive curves E'_i and E'_{i+1} is determined, as illustrated in Fig. 6. The upper and lower boundaries of the overlapping are given by:

$$E'_u = max(min(E'_i), min(E'_{i+1})) \tag{10}$$

and

$$E'_o = min(max(E'_i), max(E'_{i+1})) \tag{11}$$

Using a spline–fit for the storage modulus curves makes it possible to evaluate the inverse function in order to receive the frequency co–domain of two consecutive curves within their overlapping area:

$$f_i = (E'_i)^{-1} \tag{12}$$

and

$$f_{i+1} = (E'_{i+1})^{-1} \tag{13}$$

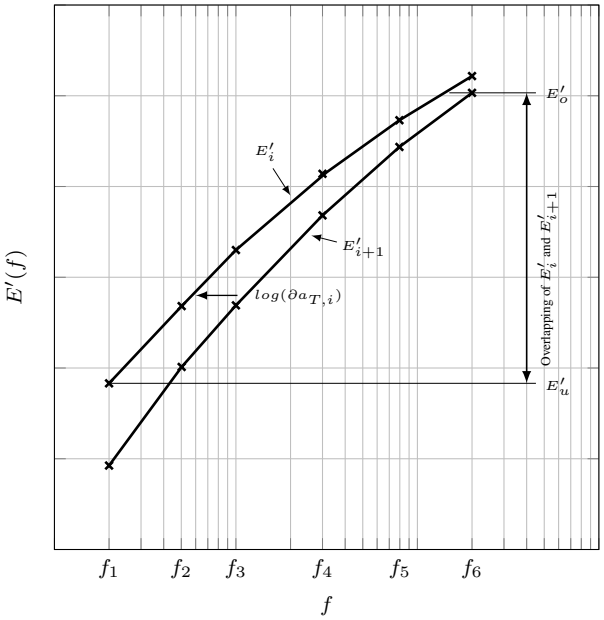

Figure 6. Overlapping of two consecutive storage modulus curves in the frequency domain

In order to shift a curve E'_{i+1} onto the $i-$th reference curve E'_i the root–mean-square of the horizontal distance between the two curves is determined, which leads to an incremental shift factor:

$$\partial\, log(a_{Ti}) = \sqrt{\frac{1}{N}\sum_{i=1}^{N}(f_{i+1} - f_i)^2} \tag{14}$$

After this the vector of the total shift factor for each curve related to the curve of the reference temperature E_{Tref} needed to develop the master curve is governed by summing the incremental shift factors as follows:

$$log(\underline{\mathbf{a_T}}) = -\sum_{i=i_{Tref}}^{n_T-1} \partial\, log(a_T(T_i, T_{i+1}|T_{ref})) + \sum_{i=1}^{i_{Tref}-1} \partial\, log(a_T(T_i, T_{i+1}|T_{ref})) \tag{15}$$

where n_T is the number of all measured temperatures $\underline{\mathbf{T}} = [T_1, ...T_{i_{Tref}}, ..., T_{n_T}]$ and i_{Tref} is the index of the reference temperature.

It should be noted that the extrapolation of the measured frequency domain by developing master curves is only done by shifting the storage modulus and the governed shift factors are applied also on the loss modulus. This can be done because storage and loss modulus are real and imaginary part of a complex quantity and they are forming a physical system for which causality is valid. Therefore, it is possible to express storage and loss modulus through each other by a Hilbert transform, which will be explained in the following and will be shown on measurement data in Sec. 5.

2.4 Hilbert Transform, Causality and the Kramers–Kronig Relation

In the following, the definitions of the Hilbert transform of a function $f(t)$, the definition of a causal function $f(t)$ and the Kramers–Kronig relation are described and set into context.

2.4.1 Hilbert Transform

The Hilbert transform (abbr. HT) is another integral transform method such as Laplace and Fourier Transform. The HT of a function $f(t)$ is defined by Hahn (1996):

$$H[f(t)] = \widetilde{f}(t) = \frac{1}{\pi} \int_{-\infty}^{\infty} \frac{f(\tau)}{t-\tau} d\tau \tag{16}$$

To be mathematically correct, the integral has to be interpreted as a Cauchy principal value, c.f. Feldman (2011). According to Feldman (2011), the HT can be interpreted physically as a linear filter, which lefts the amplitudes of the spectral components unmodified, but shifts their phases by $-\frac{\pi}{2}$. Thus $H[f(t)]$ is the convolution of $f(t)$ with $\frac{1}{\pi t}$. The impulse response function of the ideal HT is shown in Feldman (2011).

A complex signal is called an *analytic* (or *quadrature*) signal, if its imaginary part is the HT of the real part, Feldman (2011). At this point, here only the main ideas from Feldman (2011) are summarized to give just an idea on the capabilities of detecting nonlinear system behaviour by use of the HT :
The HT is a linear operator, thus the frequency response function (FRF) of a linear system is invariant under the HT. If one plots the FRF and the HT of the FRF, they should lie on top of each other (under consideration of the deviations due to measurement noise). If this is not the case, the HT indicates the presence of nonlinear system behavior. The knowledge of this statement in addition to the following statements of Sec. 2.4.2 can be used to check the validity of the assumption of linearity when having at hand experimental data.

2.4.2 Causality and the Kramers–Kronig Relation

A causal function $f(t)$ is defined as

$$f(t) = f(t) \cdot 1(t) = \begin{cases} 0 & \text{if } t < 0 \\ f(t) & \text{if } t \geq 0 \end{cases} \tag{17}$$

where $1(t)$ is the Heaviside step function, c.f. Foellinger (2011).

In the physics and engineering context causal functions are of great interest, as these functions respect the basic physical principle, that the effect cannot appear before the cause. According to Foellinger (2011), for a causal function $f(t)$ the Fourier transform reads:

$$F(\omega) = \frac{1}{2\pi} F(\omega) * F(1(t)) = \frac{1}{2\pi} F(\omega) * \left(\tfrac{1}{\mathrm{i}\omega} + \pi\delta(\omega) \right) \tag{18}$$

Conducting the convolution the results for the real and imaginary part of the Fourier transform $F(\omega)$ read:

$$\begin{aligned} \Re(\omega) &= \frac{1}{\pi} \int_{-\infty}^{\infty} \frac{\Im(v)}{\omega - v} dv \\ \Im(\omega) &= -\frac{1}{\pi} \int_{-\infty}^{\infty} \frac{\Re(v)}{\omega - v} dv \end{aligned} \tag{19}$$

These dependencies between the real and the imaginary part of a causal function $f(t)$ are called the Kramers–Kronig relations. By inspection of the form of the equations (19) above, it can be deduced, that the Kramers–Kronig relations are a special case of the HT. This further means, that the original (particularly causal) function $f(t)$ is exactly defined through either the real part $\Re(\omega)$ or the imagniary part $\Im(\omega)$, c.f. Foellinger (2011):

$$
\begin{aligned}
f(t) &= \frac{2}{\pi} \int_0^\infty \Re(\omega) cos(\omega) d\omega \\
f(t) &= -\frac{2}{\pi} \int_0^\infty \Im(\omega) sin(\omega) d\omega
\end{aligned}
\tag{20}
$$

Since the $f(t) \in \mathbb{R}$ (real function), the real part $\Re(\omega)$ has to be an even function and the imagniary part $\Im(\omega)$ has to be an odd function, c.f. Foellinger (2011).

For practical considerations, especially in terms of validating the causality and linearity of the measured data $E'(\omega)$ and $E''(\omega)$, the following approximations of the Kramers-Kronig relations can be utilized:

$$
\begin{aligned}
E'(\omega) &= -\frac{\omega \cdot 2}{\pi} \left(\frac{d[E''(u)/u]}{d \ln u} \right)_{u=\omega} \\
E''(\omega) &= \frac{2}{\pi} \left(\frac{dE'(u)}{d \ln u} \right)_{u=\omega}
\end{aligned}
\tag{21}
$$

By these equations the Kramers-Kronig relation can be approximated under certain conditions in this simple manner. For further details on the conditions and the deduction of these approximations see Booij and Thoone (1982).

3 Existing Methods from Literature and Delimitation of the own Methodology

In literature different existing methods can be found regarding the estimation of the parameters of a Prony–series representation of viscoelastic material behaviour. For fitting experimental data in the frequency domain many researchers have proposed different methods, mainly upon least squares approaches. The methods proposed so far can be categorized into methods with Tikhonov regularization techniques (Elster et al. (1992); Honerkamp and Weese (1989)), maximum entropy methods (Elster and Honerkamp (1991)), linear regression with regularization and additional constraints (Mead (1994)), nonlinear optimization methods (Baumgaertel and Winter (1989); Kuntsche (2015)) and windowing methods (Tschoegl and Emri (1993); Emri and Tschoegl (1994, 1995)). Orbey and Dealy (1991) compared some of the mentioned methods. The difficulties of the methods lie in the ill-posed nature of the problem, which has been discussed in detail by Honerkamp (1989). For reasons of brevity in this paper we focus on two different methodologies, one is the collocation method described by Tschoegl (1989) and the other one is an unregularized least squares approach by Kuntsche (2015), as this was the first applying it in the field structural engineering.

3.1 Method by Tschoegel

Tschoegl (1989) suggests the basic methodology upon which we build our derivations. The main difference between the method of Tschoegl (1989) and the method proposed here is, that in Tschoegl (1989) the "stiffness matrices" for the storage and loss moduli are introduced separately and without a physical interpretation of the influence length, as we did in section 2.2.2. The main ideas of the method are summarized in the following:

- Storage and loss modulus are treated separately in a stiffness matrix for each part,
- the stiffness matrices for storage and loss modulus are square and therefore invertible but the solution does not take into account measurement uncertainties through the right hand side (vector of collected data),
- the solution of the system of linear equations is done without restrictions, thus negative E_k are possible but do violate physical meanings,
- the fit is either in the storage or the loss modulus but not combined,
- there is no guidance for the complexity (number of elements) of the Prony–series coming from the data at hand,

- the model complexity K is assumed to be an even number,
- the fit in the storage modulus respects the scaling property $\sum_{k=1}^{K} \widehat{E}_k = E_0 - E$ but the fit in the loss modulus does not.

3.2 Method by Kuntsche

Kuntsche (2015) introduces a two–step procedure in which an initial set of parameters of the Prony series is first estimated by a genetic algorithm. These parameters are then used as a start vector in a global optimization in the second step. According to Kuntsche (2015) the highly non–linear optimization problem with several constraints can be simplified by fixing the relaxation times which leads to a linear optimization problem. This can be done by choosing one single Maxwell element for each decade in the frequency domain. Therefore, the unknown model parameters can be reduced from $2\,n+1$ to $n+1$, where n is the number of frequency decades. The essential steps within the procedure developed by Kuntsche (2015) are summarized in the following:

- reducing the number of unknown parameters by choosing the number of Maxwell–Elements (one element for each frequency decade to be described) and therefore fixing the relaxation times,
- guess of an initial set of parameters by using a genetic algorithm (random),
- starting a global optimization by minimizing the objective function

$$f \;=\; \sum_{j=1}^{m} [(log(E'(\omega_j)) - log(\widetilde{E}'(\omega_j)))^2 + 10 \cdot (log(E''(\omega_j)) - log(\widetilde{E}''(\omega_j)))^2],$$

  which is the error sum of squares between model and experimental data.

3.3 Method GUSTL

Here we give a brief statement of commons and differences of our method GUSTL in comparison to the existing methods.

- Storage and loss modulus are treated simultaneously by combining the "stiffness matrices" for each part in a "global stiffness matrices" (thus the information of the storage and the loss part are both considered),
- in contrast to Tschoegl (1989) the "global stiffness matrix" considers both, the storage and the loss modulus and is thus not square anymore, hence a nonnegative least–squares solution algorithm is used to enforce physical meaningfulness of the obtained results,
- at this stage GUSTL does not take into account measurement uncertainties through the right hand side (vector of collected data) but will do so in a further extension,
- at this stage GUSTL does also not present a guidance for the complexity (number of elements) for the complexity K of the Prony series coming from the data at hand,
- the model complexity K can be chosen arbitrarily even or odd,
- the fit of the Prony series by GUSTL respects the scaling property $\sum_{k=1}^{K} \widehat{E}_k = E_0 - E$ in both, the storage and the loss modulus,
- in contrast to Kuntsche (2015) GUSTL is way faster (in terms of wall-clock time) than the two stage procedure. GUSTL needs only seconds while the method by Kuntsche needs several hours. Furthermore the estimation of the Prony–series by GUSTL can be used as a good initial guess for the second step (global search optimization) avoiding the time-consuming use of a genetic algorithm (which moreover treats the problem as a random one without taking into account the physical meanings).

4 Deduction of the Method GUSTL

In this section we want to present a fast and accurate method of either determining the Prony–series in one step or to provide a good initial point for further (non–linear) Least–Squares solver.

According to Honerkamp (1989) the (non–linear) Least-Squares problem suffers from:

- being ill–conditioned,
- solution may be a local minimum,
- huge numerical effort to obtain the global minimum (is in general not guaranteed to be found).

In order to cope with the problems mentioned before, it has to be pointed out, that in the case of fitting a Prony series to the data, this is not a problem of "pure regression" as there is some physics behind the data, which restrict the problem. In section 2.2.2 we therefore did some considerations on the influence lengths of a single Maxwell element in the storage and loss modulus. We want to emphasize, that our proposed method GUSTL is a collocation method, which uses a numerical method which considers the physically sensible restrictions of the problem structure.

The main properties are:

- derivation of stiffness matrices for the storage and loss modulus, which take into account the mutual influence of the Maxwell elements,
- combining the collocations for the storage and loss modulus parts into one global stiffness matrix $\mathbf{K_{global}}$ of the whole fitting process,
- solving the resulting system of linear equations numerically by a non–negative Least–Squares routine.

4.1 Basic Assumptions and Systematology

The deduction for GUSTL is in general applicable to all response functions and is in principle a collocation method such as those suggested by Tschoegl (1989). We stick to the nomenclature introduced and adapted by Tschoegl (1989) as this was the basis for the following.

With GUSTL we want to derive a system of linear equations, which possesses the following form:

$$\underline{\underline{\mathbf{K}}}_{\mathbf{global}} \cdot \left[\underline{\boldsymbol{G}}\right] = \left[\underline{\tilde{\boldsymbol{E}}}\right] \Leftrightarrow \begin{bmatrix} \underline{\underline{\boldsymbol{K}}}_{Store} \\ - - - - \\ \underline{\underline{\boldsymbol{K}}}_{Loss} \\ - - - - \\ \underline{\mathbf{1}} \end{bmatrix} \cdot \left[\boldsymbol{G}\right] = \begin{bmatrix} \underline{\tilde{\boldsymbol{E}}}'(\omega) \\ - - - - \\ \underline{\tilde{\boldsymbol{E}}}''(\omega) \\ - - - - \\ \tilde{E}_0 - \tilde{E} \end{bmatrix} \tag{22}$$

The last line in Eq. 22 is introduced in the stiffness matrix to enforce the satisfaction of the scaling $\sum_{k=1}^{K} \widehat{E}_k = E_0 - E$. We suppose, that the raw experimental observations have been shifted to a suitably smooth master curve in the storage modulus and are made at steps logarithmic equally spaced frequency scale. The task now is to obtain a generalized Maxwell model of complexity K. The data thus are gathered at

$$\omega_j = 10^{m+j}, \qquad j = \frac{\omega_{fin} - \omega_{start}}{K} \tag{23}$$

The beginning of the ω–axis is at $\omega_{start} = 10^m$ where the first observation is made and it ends at $\omega_{fin} = 10^{m+K}$.

The index notation of Eq. 22 reads:

$$\begin{bmatrix} K_{Store,jk} \\ - - - - \\ K_{Loss,jk} \\ - - - - \\ 1 \end{bmatrix} \cdot \left[\widehat{E}_k\right] = \begin{bmatrix} \tilde{E}'(\omega_j) \\ - - - - \\ \tilde{E}''(\omega_j) \\ - - - - \\ \tilde{E}_0 - \tilde{E} \end{bmatrix} \tag{24}$$

Tschoegl (1989) cites Schapery which has introduced a relation of the relaxation times τ_k, to the frequencies ω_k through the equation:

$$\omega_k = \frac{1}{a \cdot \tau_k} = \frac{1}{a \cdot 10^{m+k}}, \qquad k = \frac{\omega_{fin} - \omega_{start}}{K} \tag{25}$$

Tschoegl (1989) mentions, that a is a proportionality constant, which has to be chosen in a "suitable way" but leaves the choice open and gives the hint, that for different values of a different sets of $\boldsymbol{G}$'s are obtained, so that the choice is somehow "arbitrary". Tschoegl (1989) sets $a = 1$ in his considerations.

At this point we want to mention, that our understanding of the parameter a is, that a is not arbitrary but can be interpreted as the horizontal shift factor $a_T(T)$ when dealing with the raw data, which are collected at the same test frequencies for different temperatures. A method of incorporating the shift–procedure in "GUSTL" based on this interpretation will be deduced in a follow up publication to this paper.

For the method GUSTL as presented in this paper, we will consider $a = 1$, as we already constructed the master curve as described in Sec. 2.3.

4.1.1 Derivation of the Stiffness Matrix for the Storage Modulus $\underline{\underline{\mathbf{K}}}_{Store}$

The "stiffness matrix" for the Storage modulus $\underline{\underline{\mathbf{K}}}_{Store}$ can be directly obtained by evaluating the basis functions of the storage modulus $\underline{\mathbf{b}}'_k$. It possesses the form:

$$K_{Storage,jk} = \frac{1}{1 + a^2 \frac{\omega_k^2}{\omega_j^2}} = \frac{1}{1 + a^2 100^{k-j}} \tag{26}$$

An alternative way of construction in case of one Maxwell element per decade can be achieved directly from the considerations in 2.2.2 about the influence lengths using a lower triangular matrix, c.f. Fig 7. Here we present the MATLAB code therefore:

```
K_store=tril(ones(N,N),-2)+diag(ones(N,1)).*0.5+diag(ones(N-1,1),-1).*0.5;
```

The scaling condition $\sum_{k=1}^{K} \widehat{E}_k = E_0 - E$ introduces an extra line with ones into $\underline{\underline{\mathbf{K}}}_{Store}$, this line is shifted to the very last line in the "global stiffness matrix" $\underline{\underline{\mathbf{K}}}_{global}$.

For $K = 6$ the "stiffness matrix" for the storage modulus $\underline{\underline{\mathbf{K}}}_{Store}$ becomes:

$$\left[\begin{array}{cccccc} 0.500 & 0.000 & 0.000 & 0.000 & 0.000 & 0.000 \\ 1.000 & 0.500 & 0.000 & 0.000 & 0.000 & 0.000 \\ 1.000 & 1.000 & 0.500 & 0.100 & 0.000 & 0.000 \\ 1.000 & 1.000 & 1.000 & 0.500 & 0.000 & 0.000 \\ 1.000 & 1.000 & 1.000 & 1.000 & 0.500 & 0.000 \\ 1.000 & 1.000 & 1.000 & 1.000 & 1.000 & 0.500 \\ \hline 1.000 & 1.000 & 1.000 & 1.000 & 1.000 & 1.000 \end{array}\right] \tag{27}$$

The structure of the "stiffness matrix" for the storage modulus $\underline{\underline{\mathbf{K}}}_{Store}$ is visualized in the following figure for $K = 20$:

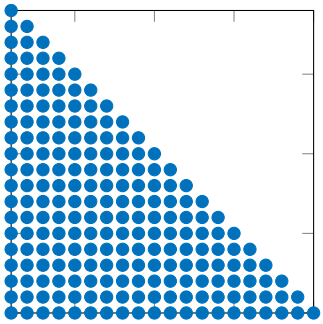

Figure 7. Principal matrix structure for $\underline{\underline{\mathbf{K}}}_{Store}$

4.1.2 Derivation of the Stiffness Matrix for the Loss Modulus $\underline{\underline{\mathbf{K}}}_{Loss}$

The "stiffness matrix" for the loss modulus $\underline{\underline{\mathbf{K}}}_{Loss}$ can also be directly obtained by evaluating the basis functions of the loss modulus $\underline{\mathbf{b}}''_k$. It possesses the form:

$$K_{Loss,jk} = \frac{1}{a\frac{\omega_k}{\omega_j} + \frac{1}{a}\frac{\omega_j}{\omega_k}} = \frac{1}{a10^{k-j} + \frac{1}{a}10^{j-k}} \tag{28}$$

An alternative way of construction in case of one Maxwell element per decade can be achieved directly from the considerations in 2.2.2 about the influence lengths using a pentadiagonal or heptdiagonal matrix, c.f. Fig 8. Here we present the MATLAB code for the heptdiagonal case (when choosing the numerical precision to be 1/1000):

```
K_loss=zeros(N,N);
K_loss=diag(ones(N,1)).*0.5+...
    diag(ones(N-1,1),-1).*1/10 + diag(ones(N-1,1),+1).*1/10+...
    diag(ones(N-2,1),-2).*1/100 + diag(ones(N-2,1),+2).*1/100+...
    diag(ones(N-3,1),-3).*1/1000 + diag(ones(N-3,1),+3).*1/1000;
```

For $K = 6$ the "stiffness matrix" for the loss modulus $\underline{\underline{\mathbf{K}}}_{Loss}$ becomes:

$$\begin{bmatrix} 0.500 & 0.100 & 0.010 & 0.001 & 0.000 & 0.000 \\ 0.100 & 0.500 & 0.100 & 0.010 & 0.001 & 0.000 \\ 0.010 & 0.100 & 0.500 & 0.100 & 0.010 & 0.001 \\ 0.001 & 0.010 & 0.100 & 0.500 & 0.100 & 0.010 \\ 0.000 & 0.001 & 0.010 & 0.100 & 0.500 & 0.100 \\ 0.000 & 0.000 & 0.001 & 0.010 & 0.100 & 0.500 \end{bmatrix} \tag{29}$$

The structure of the "stiffness matrix" for the Storage modulus $\underline{\underline{\mathbf{K}}}_{Loss}$ is visualized for $K = 20$ in the following figure:

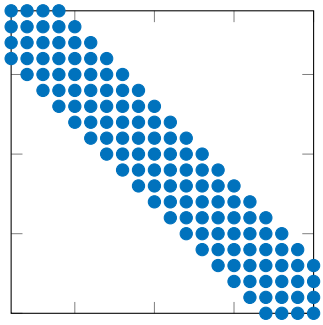

Figure 8. Principal matrix structure for $\underline{\underline{\mathbf{K}}}_{Loss}$

4.1.3 Construction of the Global Stiffness Matrix $\underline{\underline{\mathbf{K}}}_{global}$

The assembling of the "global stiffness matrix"$\underline{\underline{\mathbf{K}}}_{global}$ is straight forward out of the two parts $\underline{\underline{\mathbf{K}}}_{Storage}$ and $\underline{\underline{\mathbf{K}}}_{Loss}$:

$$\mathbf{K_{global}} = \begin{bmatrix} \underline{\underline{\boldsymbol{K}}}_{Store} \\ - - - - \\ \underline{\underline{\boldsymbol{K}}}_{Loss} \\ - - - - \\ \underline{\mathbf{1}} \end{bmatrix} \tag{30}$$

For $K = 6$ the "global stiffness matrix"$\underline{\underline{\mathbf{K}}}_{global}$ becomes:

$$\begin{bmatrix} \begin{bmatrix} 0.500 & 0.000 & 0.000 & 0.000 & 0.000 & 0.000 \\ 1.000 & 0.500 & 0.000 & 0.000 & 0.000 & 0.000 \\ 1.000 & 1.000 & 0.500 & 0.100 & 0.000 & 0.000 \\ 1.000 & 1.000 & 1.000 & 0.500 & 0.000 & 0.000 \\ 1.000 & 1.000 & 1.000 & 1.000 & 0.500 & 0.000 \\ 1.000 & 1.000 & 1.000 & 1.000 & 1.000 & 0.500 \end{bmatrix} \\ \begin{bmatrix} 0.500 & 0.100 & 0.010 & 0.001 & 0.000 & 0.000 \\ 0.100 & 0.500 & 0.100 & 0.010 & 0.001 & 0.000 \\ 0.010 & 0.100 & 0.500 & 0.100 & 0.010 & 0.001 \\ 0.001 & 0.010 & 0.100 & 0.500 & 0.100 & 0.010 \\ 0.000 & 0.001 & 0.010 & 0.100 & 0.500 & 0.100 \\ 0.000 & 0.000 & 0.001 & 0.010 & 0.100 & 0.500 \end{bmatrix} \\ \begin{bmatrix} 1.000 & 1.000 & 1.000 & 1.000 & 1.000 & 1.000 \end{bmatrix} \end{bmatrix} \tag{31}$$

4.1.4 Derivation of the Right Hand Side $\underline{\tilde{\mathbf{E}}}$

The right hand side is mainly the vector of the measured data in the storage and loss modulus at the frequencies ω_j and in the last line the incorporation of the constraint $\sum_{k=1}^{K} \widehat{E}_k = E_0 - E$. This scaling constraint indeed can be solely be derived from the storage modulus as there exist (theoretically) limits in the absolute values of the storage modulus, namely $\lim_{\omega \to 0} E'(\omega) = E$ and $\lim_{\omega \to \infty} E'(\omega) = E_0$.

Thus the right hand side reads:

$$\begin{bmatrix} \tilde{E}'(\omega_j) \\ - - - - \\ \tilde{E}''(\omega_j) \\ - - - - \\ \tilde{E}_0 - \tilde{E} \end{bmatrix} \tag{32}$$

Alternatively one migth use the normalized version of Eq. 32:

$$\begin{bmatrix} \frac{\tilde{E}'(\omega_j)}{\tilde{E}_0 - \tilde{E}} \\ - - - - \\ \frac{\tilde{E}''(\omega_j)}{\tilde{E}_0 - \tilde{E}} \\ - - - - \\ 1 \end{bmatrix} \tag{33}$$

In the general case it is only possible to guess $\tilde{E}_0$ and $\tilde{E}$ from the master curve of the storage modulus. The solution for the coefficient vector $\underline{\boldsymbol{G}}$ can highly be affected by this guess as it may be contaminated by measurement noise.

4.1.5 The non–negative Least Squares Algorithm

Due to the physical meaning of the entries of the coefficient vector $\underline{\boldsymbol{G}}$ a non–negativity constraint has to be introduced in the solution process of the system of linear equations (22). In mathematical optimization, this problem is known as the non–negative least squares (NNLS), which is a constrained version of the (ordinary) least squares problem. Here the coefficients $\underline{\mathbf{G}}$ are not allowed to become negative. Formally, we want to find a solution of the problem:

$$\underset{\underline{\mathbf{G}}}{\operatorname{argmin}} \left\| \underline{\underline{\mathbf{K}}}_{global} \cdot \underline{\mathbf{G}} - \underline{\tilde{\mathbf{E}}} \right\|_2 \tag{34}$$

subject to

$$\underline{\mathbf{G}} \geq \underline{\mathbf{0}} \tag{35}$$

In the context of the examples in the latter we use the MATLAB built–in solver "lsqnonneg", which uses the algorithm described in Lawson and Hanson (1974). According to Lawson and Hanson (1974), the algorithm consists of a main loop and an inner loop. The algorithm starts with a set of possible basis vectors (positive entries) and computes the associated dual vector $\underline{\lambda}$. It then selects the basis vector corresponding to the maximum value in lambda to swap it out of the basis in exchange for another possible candidate. This continues until $\underline{\lambda} \leq \underline{\mathbf{0}}$.

This problem always has a solution but it is non-unique if the rank of $\underline{\underline{\mathbf{K}}}_{global}$ is less than complexity K. According to Lawson and Hanson (1974) it can be proved that this algorithm converges in a finite number of iterations.

4.1.6 Solution Algorithm

The solution procedure is explained in principle by the following algorithm flowchart

Algorithm 1 GUSTL algorithm

1: $K \leftarrow$ complexity of the Generalized Maxwell Model
2: *Building of* K_{Store}*:*
3: $K_{Storage,jk} = \frac{1}{1+a^2 \frac{\omega_k^2}{\omega_j^2}} = \frac{1}{1+a^2 100^{k-j}}$
4: *Building of* K_{Loss}*:*
5: $K_{Loss,jk} = \frac{1}{a\frac{\omega_k}{\omega_j} + \frac{1}{a}\frac{\omega_j}{\omega_k}} = \frac{1}{a10^{k-j} + \frac{1}{a}10^{j-k}}$
6: *Assembling of* K_{global}*:*
7: $K_{global} = [[K_{Store}; K_{Loss}]; ones(1, K)]$;
8: *Assembling of Right Hand Side:*
9: $data_E = [data_{E,Store}; data_{E,Loss}; (E_0 - E)]/(E_0 - E)$;
10: *Solution:*
11: $G \leftarrow K_{global} \cdot G = data_E$ solved by non–negative least squares, c.f. (Lawson and Hanson (1974));

5 Examples

The methodology of GUSTL was used to investigate very different viscoelastic materials which are common in the field of structural engineering. The first example described in the following is a coated carbon textile reinforcement for light–weight concrete structures. The second example for which GUSTL was applied successfully is a PVB–interlayer for laminated safety glass.

5.1 Coated Carbon Textile Reinforcement for Concrete Structures

The first material investigated is a carbon textile grid which is used as reinforcement material for light–weight concrete structures. The textile fabric is coated with an epoxy resin and therefore shows typical viscoelastic material behaviour. Especially when it is used as reinforcement for concrete layers to strengthen existing bridges the knowledge of the time respectively frequency and temperature dependent axial stiffness is of great interest because loadings caused by temperature and cyclic excitation play an important role regarding bridge engineering.

In order to investigate the viscoelastic properties of the carbon reinforcement DMA experiments were conducted in a three–point–bending mode in a temperature range $T \in [-40, 180]°C$ in steps of $2°C$ and with six different frequencies spaced logarithmically equidistant in a range of $f \in [0.2, 20]Hz$. The results of the DMA tests are shown in fig. 9.

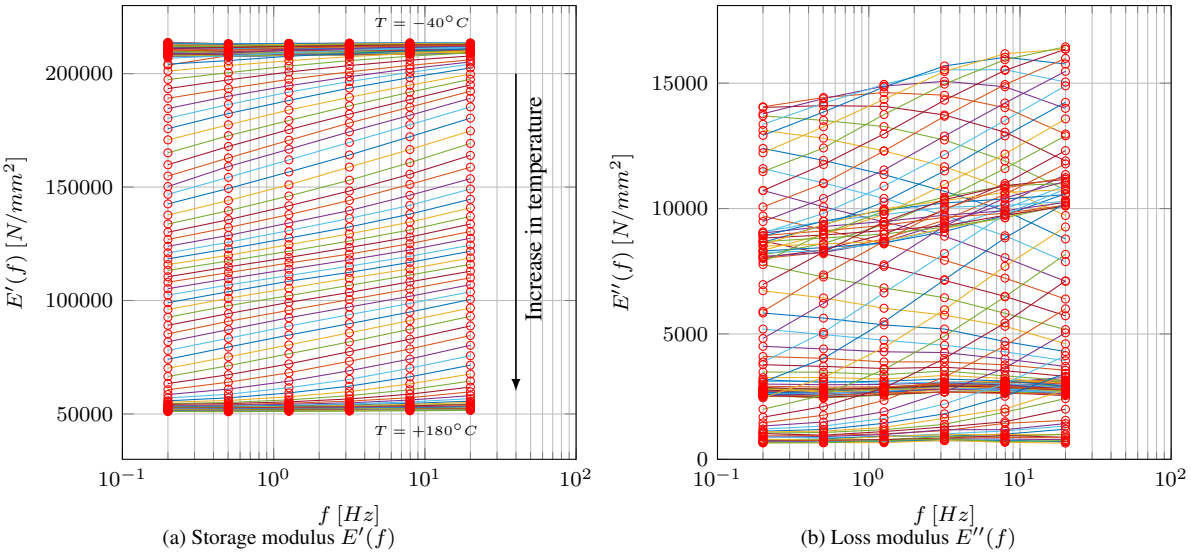

(a) Storage modulus $E'(f)$ (b) Loss modulus $E''(f)$

Figure 9. Isothermal Storage and Loss modulus curves within the tested frequency domain

According to the experimental data the glass transition takes place in the region of $50°C$ to $130°C$ (depending on the definition of the evaluation method of T_g used) which is typical for epoxy resins.

In order to obtain the master curve by horizontally shifting the data on the frequency axis the procedure described in sec. 2.3 was used to develop the master curve at a reference temperature of $T_{ref} = 20°C$. The obtained horizontal shift factors a_T are given in the following graph:

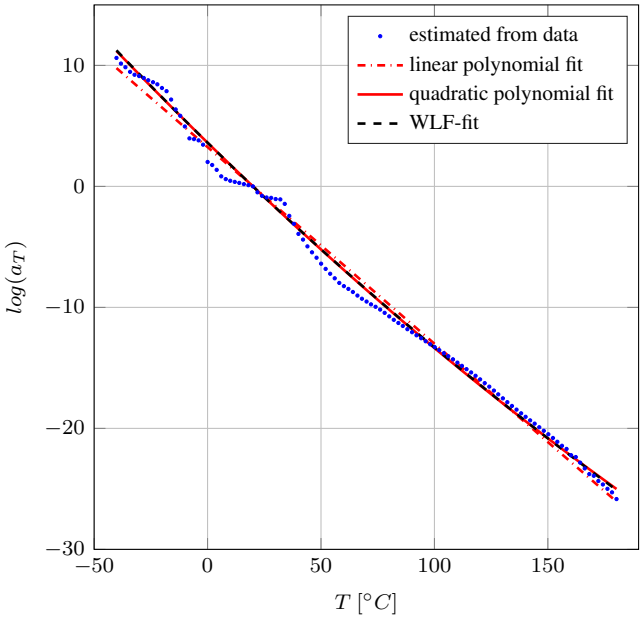

Figure 10. Logarithmic shift factor a_T over temperature T

For the time–temperature–equivalence principle we fitted the Williams–Landel–Ferry (WLF) equation, a linear and a quadratic polynomial to the data of $log(a_T)$ against T. We obtained the functional forms for the horizontal shift factors a_T via a constrained fit to ensure $log(a_T) = 0$ (resp. $a_T = 1$) for $T = T_{ref}$. As one can see in Fig. 10, any of the models is suitable to describe the shift factors estimated from the experimental data.

The derived master curve for the storage modulus is shown in Fig. 12. As described in sec. 2.4 the principle of causality is valid and therefore the shift factors estimated for the storage modulus can be used to determine the master curve for the loss modulus which is illustrated in Fig. 13. In order to govern the Prony–series for the investigated material the introduced method GUSTL is used for estimating an initial set of model parameters in the first place.

The frequency axis is discretized with 32 elements in a range of $f \in [10^{-22}, 10^{0}]Hz$. In Fig. 11 the distribution of the coefficients E_i of the parameters is given. The coefficients were obtained with an non–negative least squares estimation as well as with the pseudo inverse (ordinary least-squares algorithm) as shown in Fig. 11. The estimated coefficients by GUSTL were used as a initial guess for the global search method (c.f. Kuntsche (2015) as well as Sec. 3).

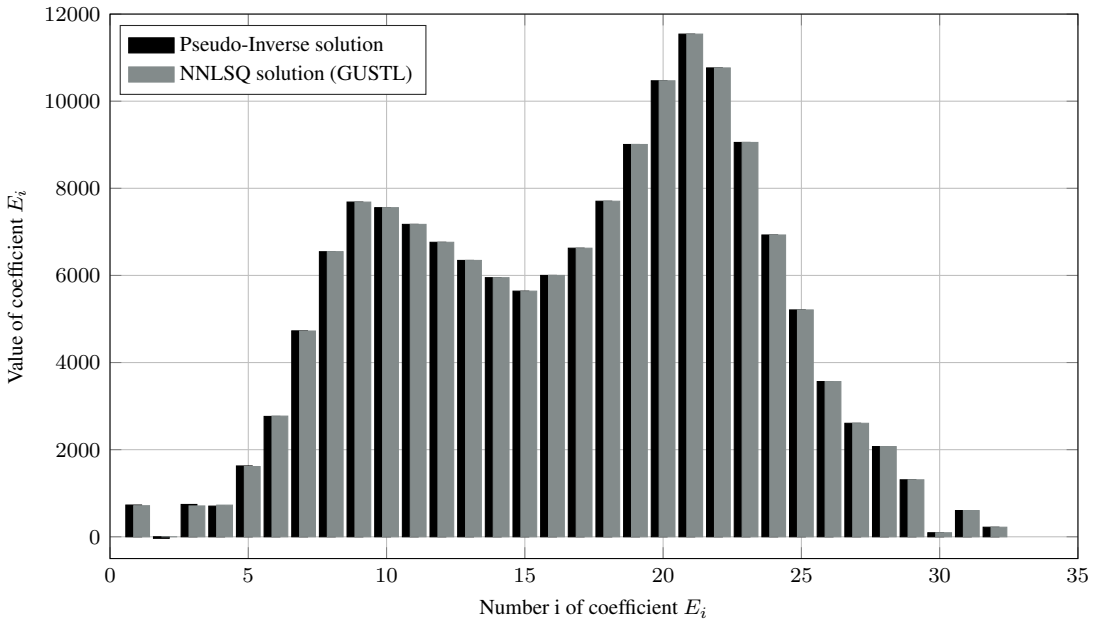

Figure 11. Coefficients E_i of the initial guess of the parameters

The resulting storage and loss modulus obtained with the methodology of GUSTL in comparison to an ordinary least–squares approximation using the global search method is illustrated in Fig.12 and 13. As one can see from the figures GUSTL delivers already a very good approximation of the experimental data while the following least squares approach leads to a more inaccurate estimation especially in the storage modulus $E'(\omega)$. This is not surprising as the global search method does not take into account the physical behavior of the Prony bases vectors (c.f. 2.2.2) of the problem under investigation.

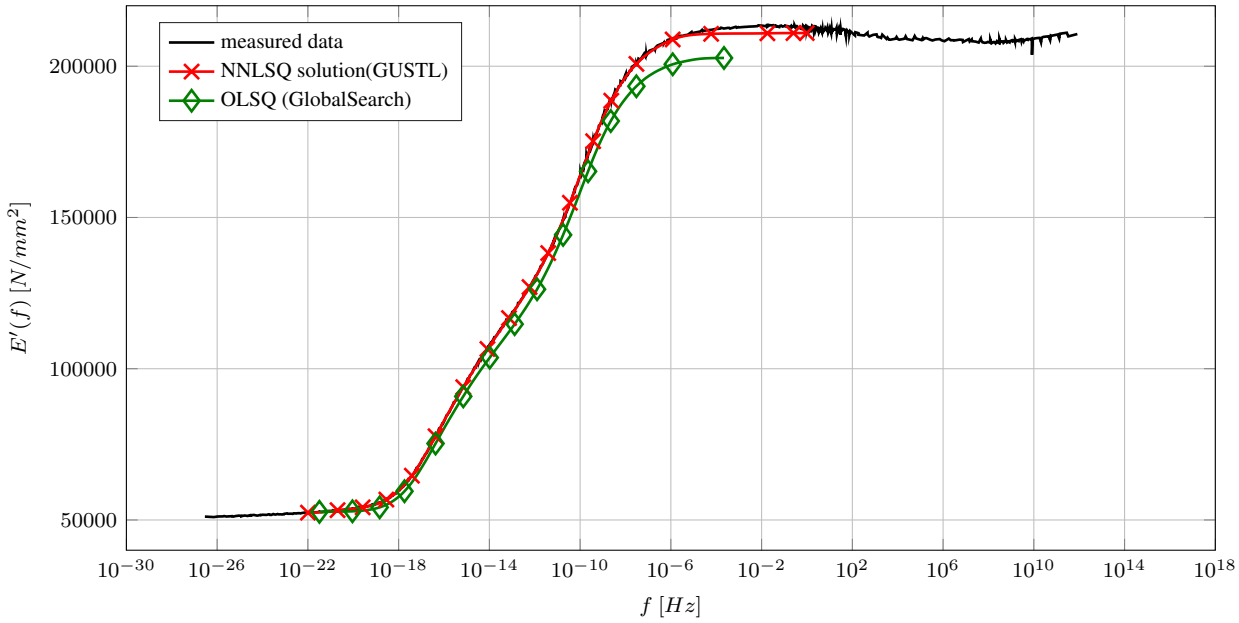

Figure 12. Storage modulus

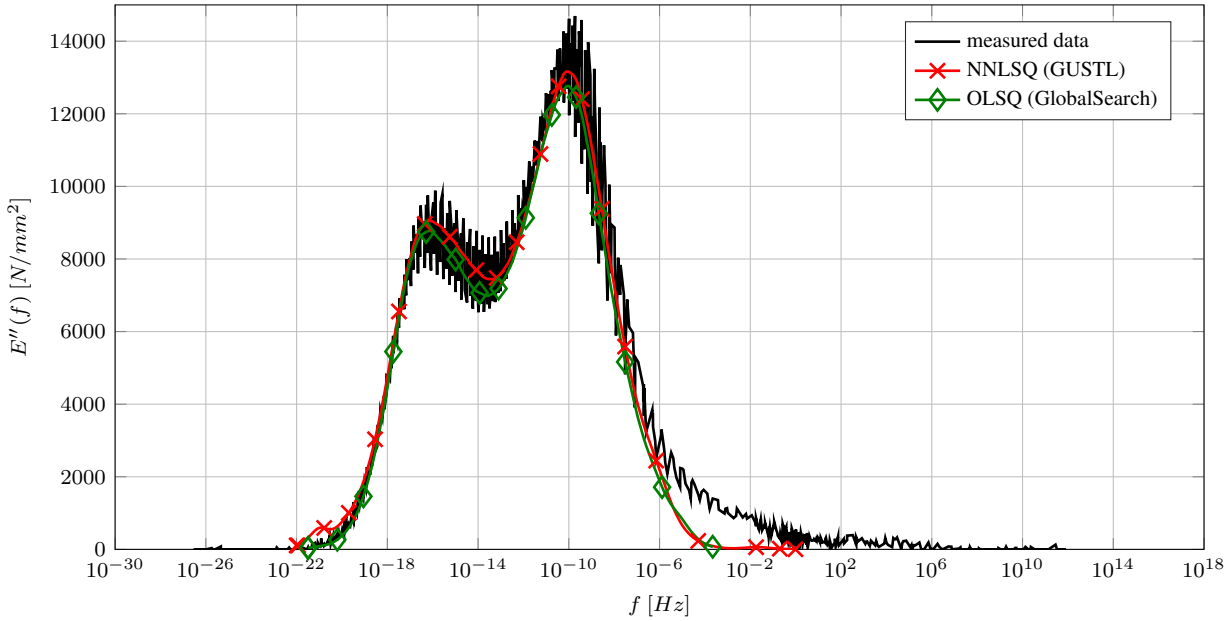

Figure 13. Loss modulus

A comparison of the distribution of the coefficients obtained with GUSTL and the global search method is shown in Fig. 14.

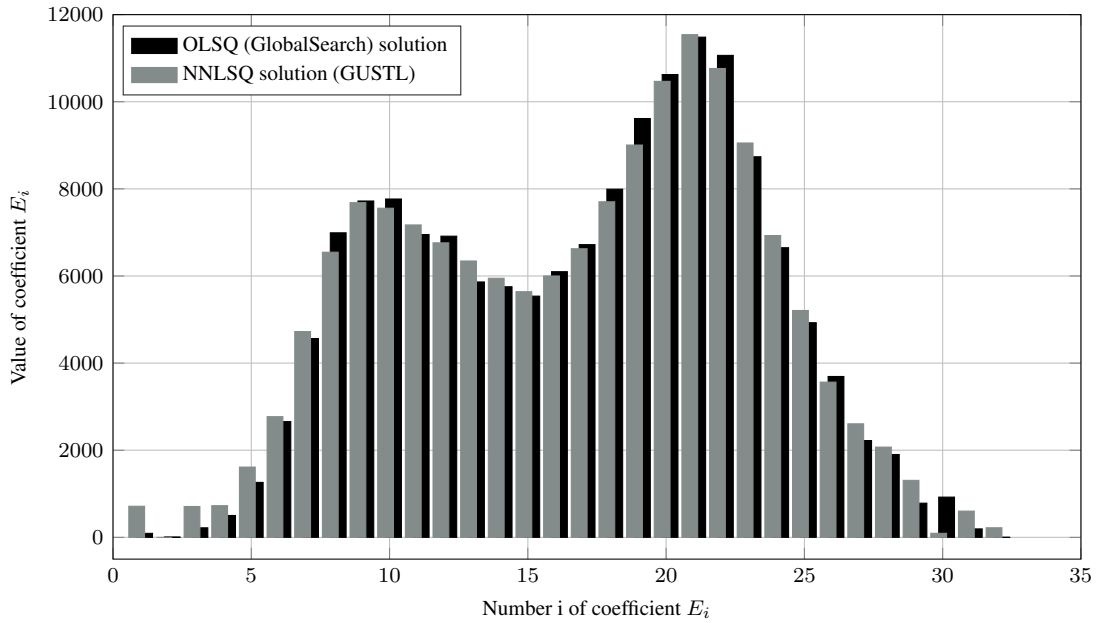

Figure 14. Coefficients E_i of the finial fit

In order to check the validity of linear viscoelastic material behaviour the loss modulus was derived by an approximation of the Kramers–Kronig–Transform (as described in sec. 2.4) using the derivative of the storage modulus. Fig. 15 shows the Kramers–Kronig approximation in comparison to the measured data. From this we can conclude that the assumptions of linear viscoelasticity are fullfilled.

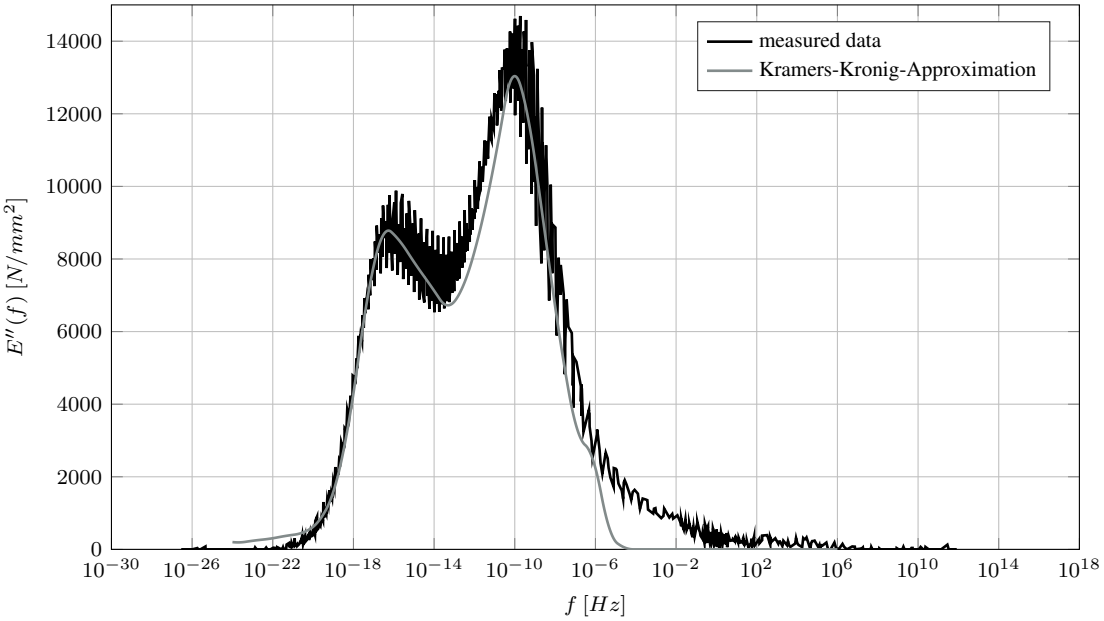

Figure 15. Check on Linearity: Kramers–Kronig–Transfrom of $E'(f)$ against the loss modulus $E''(f)$

5.2 PVB–interlayer for Laminated Glass

The second example deals with the experimental evaluation of the linear viscoelastic material behaviour of a stiff Polyvinylbutyral (PVB) interlayer, which is used as an interlayer material in laminated safety glass in structural facade engineering applications. The knowledge of the time and temperature dependent shear modulus of the interlayer material is of great practical interest, as this allows an optimized structure in terms of sustainability and economic efforts. The glass transition T_g of PVB is in general in the range of $20°C - 70°C$, depending on the definition of the evaluation method of T_g used (Kuntsche (2015)), and does depend strongly on the chemistry of the specific PVB. The T_g of PVB at hand lies in the region of $46°C$, c.f. Eastman (2015).

The DMA tests were conducted on a specimen in torsional mode in a temperature range $T \in [-20, 70]°C$ in steps of $5°C$ and a frequency range $f \in [0.02, 20]Hz$ (spaced logarithmically equidistant in 15 points).

The results of the DMA tests are shown in Fig. 16.

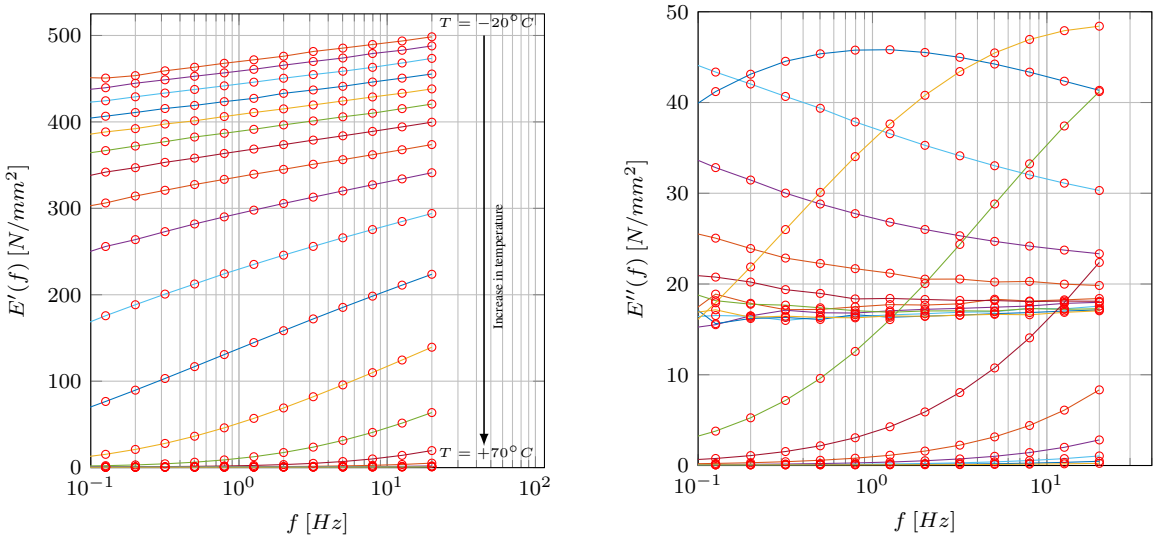

(a) Storage modulus $E'(f)$

(b) Loss modulus $E''(f)$

Figure 16. Isothermal storage and loss modulus curves within the tested frequency domain

A horizontal shifting procedure was performed by using the method described in Sec. 2.3 to obtain the master curve for a reference temperate $T_{ref} = 20°C$. The obtained horizontal shift factors a_T are given in the following graph:

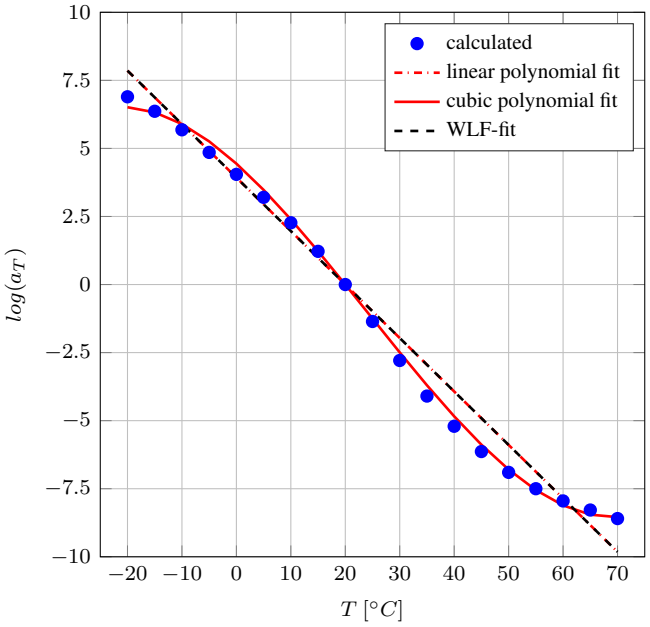

Figure 17. Logarithmic shift factor a_T over temperature T

For the time–temperature–equivalence principle we fitted the Williams–Landel–Ferry (WLF) equation, a linear and a cubic polynomial to the data of $log(a_T)$ against T. We obtained the functional forms for the horizontal shift factors a_T via a constrained fit to ensure $log(a_T) = 0$ (resp. $a_T = 1$) for $T = T_{ref}$. As to expect, the WLF does not fit very well because with $T_{ref} = 20°C$ we are away from the T_g, while the cubic polynomial seems to fit the a_T the best. The fit of the cubic polynomial was motivated in the original derivation of the WLF equation, as this is another approximation of the temperature dependence of the relaxation behaviour of the PVB. The disadvantage of using a cubic polynomial is, that it is not globally convex over the whole temperature range, hence the use of the polynomial for obtaining suitable a_T is restricted to the tested temperature range.

After the master curve construction we use GUSTL to find the estimation of the Prony–series of the material. The frequency range is chosen to be $f \in [10^{-10}, 10^{7}]Hz$. We discretize the freqency axis with 34 elements, which is a really narrow sampling. On the other hand, we can see from the storage modulus (Fig. 16a), that E_0 is not yet reached within the frequency range of the master curve as in the high terminal frequency range still a slope in the storage modulus master curve is clearly observable. Hence the E_0 has to be estimated from an extrapolation of the data. As we will truncate the Prony series at $f = 10^6$ because of a lack of data, in this case $E_0 = 498.46MPa$ is set.

The distribution of the coefficients E_i obtained via GUSTL in comparison to an ordinary least squares estimation via the pseudo inverse is given in the following figure:

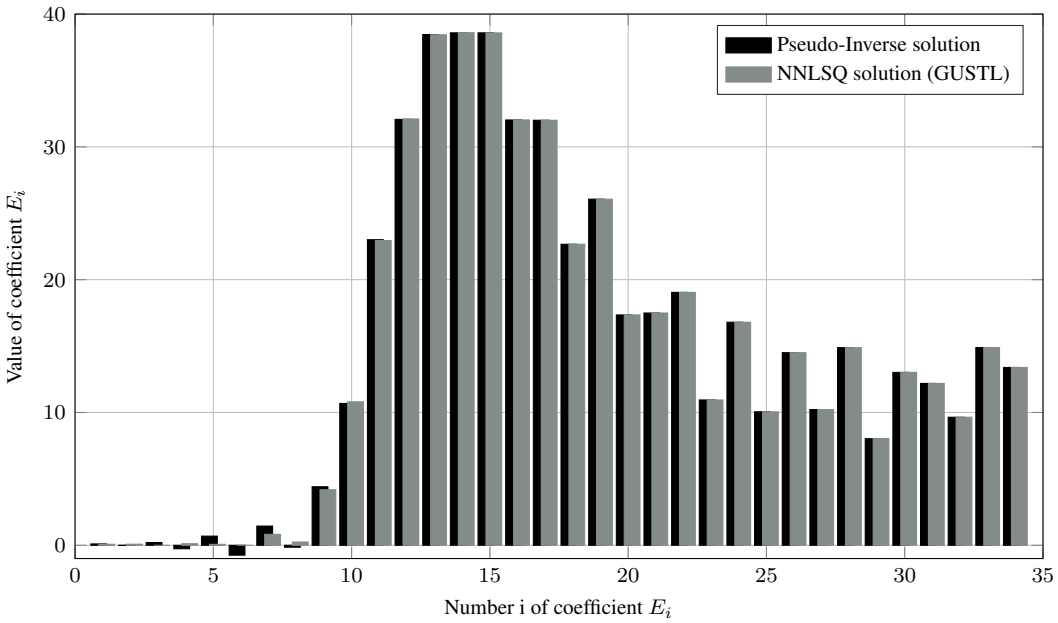

Figure 18. Coefficients E_i of the initial guess of the parameters

The resulting storage and loss moduli obtained via GUSTL in comparison to the ordinary least–squares estimation from the global search method are given in the following figures. From Fig. 19 GUSTL as well as the global search method deliver a comparable result. At this point it is worth mentioning, that even the accuracy of both methods is almost equivalent, the solution for the coefficients when using GUSTL is within milliseconds whereas the solution found by the global search may take up to minutes or even hours.

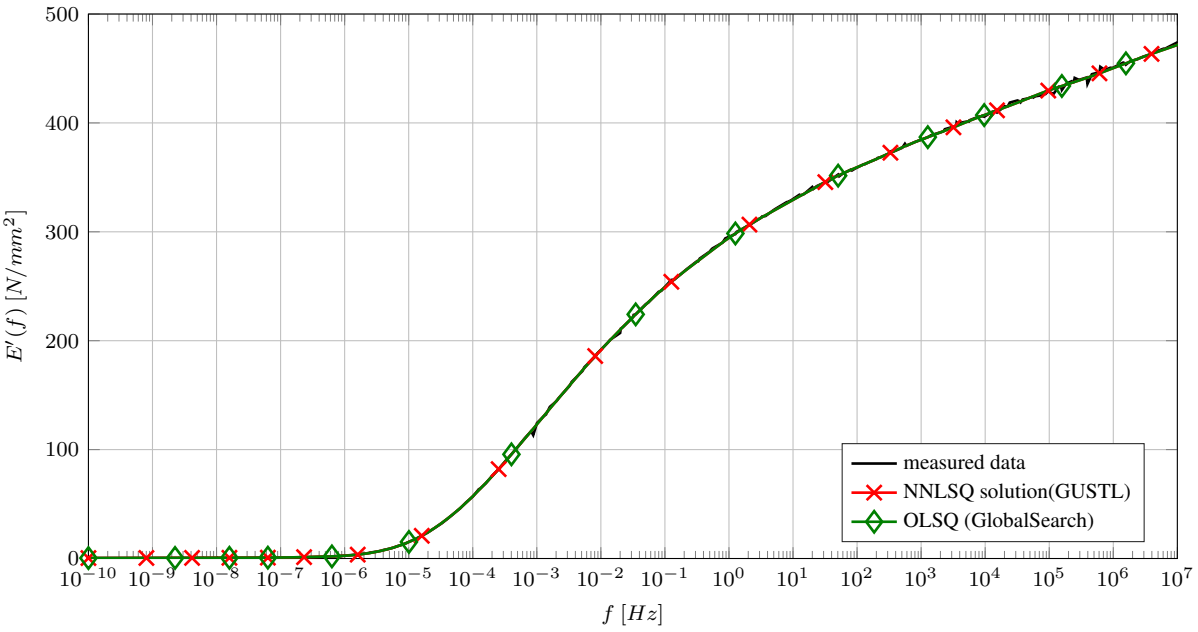

Figure 19. Storage modulus

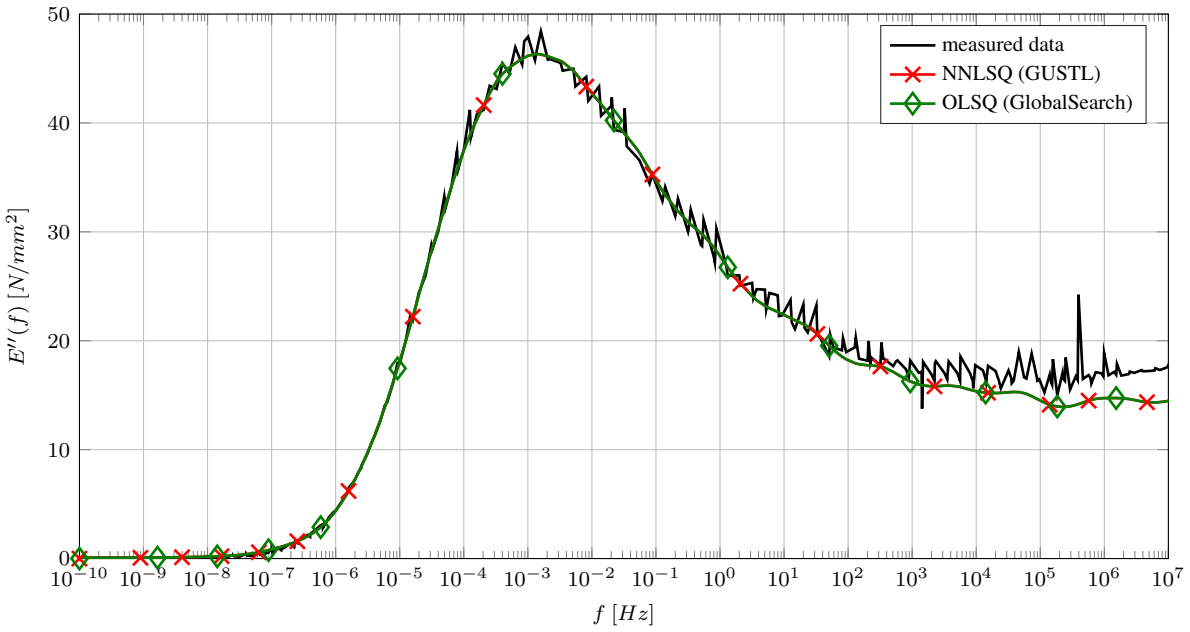

Figure 20. Loss modulus

The distribution of the coefficients E_i obtained via GUSTL in comparison to the ordinary least squares estimation by the global search method is given in the following figure:

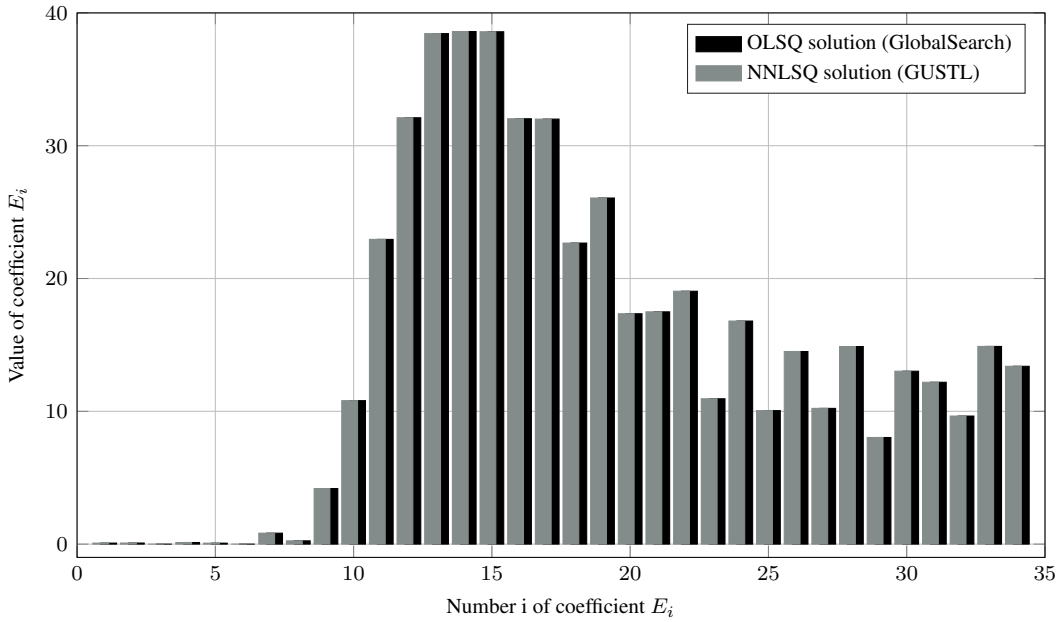

Figure 21. Coefficients E_i of the finial fit

Finally, we do an investigation on the linearity of the obtained data via a double–check of the approximate Kramers–Kronig–Transform (c.f. Eq. 21) of the obtained storage modulus $E'(f)$ against the obtained loss modulus $E''(f)$:

From Fig. 22 we conclude, that the measurements were taken in a regime, where the material behaves linear, thus the assumptions for using the obtained Prony series in the context of a linear viscoelastic material model are fulfilled.

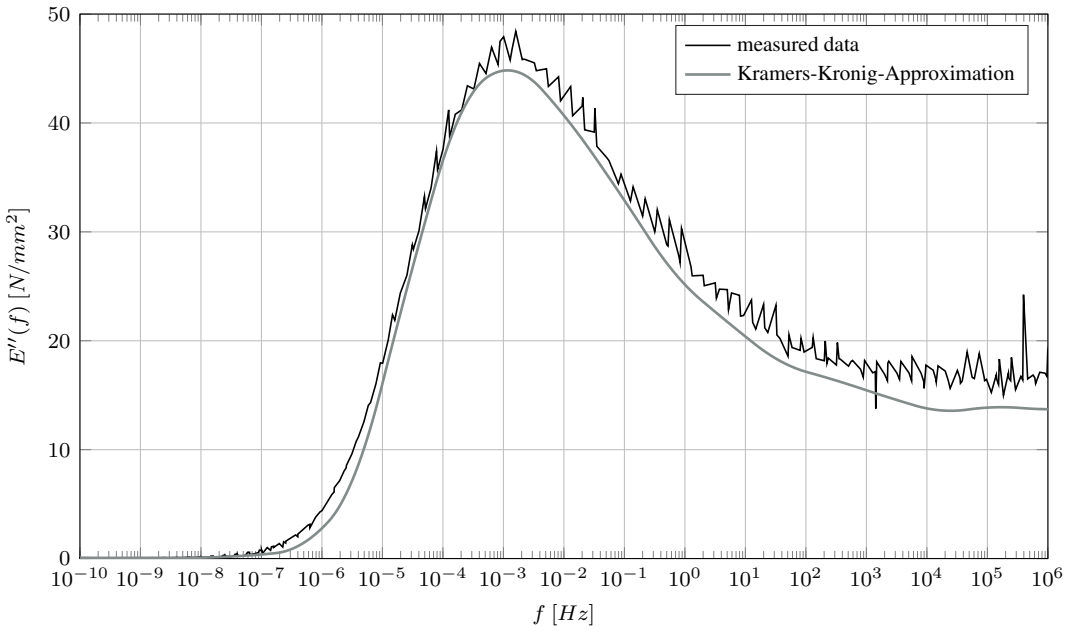

Figure 22. Check on Linearity: Kramers–Kronig–Transfrom of $E'(f)$ against the Loss modulus $E''(f)$

6 Summary, Conclusion and Outlook

In this paper we introduced and deducted a fast and accurate collocation method called GUSTL in order to estimate the coefficients $\underline{\mathbf{G}}$ of the Prony–series for a generalized Maxwell model of complexity K when having at hand data coming from DMA tests or to provide at least a sensible starting point to further least squares algorithms for determining final coefficients of the Prony–series. We investigated the structure of the stiffness matrices of the storage and loss modulus and motivated this by inspection of the "influence lengths" of a single Maxwell element. The main advantages such as numerical efficiency et al. over existing methods have been highlighted. We presented the applicability of the method against two examples from state–of–the–art research in structural civil engineering.

At last, we want to highlight further extensions of the method GUSTL, which will be presented in papers to come:

- direct processing of the master curve out of measurement data by GUSTL by incorporating the time–temperature–superposition principle
- rigorous uncertainty quantification in the processes of model building and data capturing by using a Bayesian framework for GUSTL
- deduction of the predictive distributions of the material response for different temperatures and frequencies
- further elaboration of the methods for the detection of nonlinear material behavior using the Hilbert Transform (HT)

Literatur

Baumgaertel, M.; Winter, H. H.: Determination of discrete relaxation and retardation time spectra from dynamic mechanical data. *Rheologica Acta 28*, pages 511–519.

Bergström, J.: *Mechanics of Solid Polymers. Theory and Computational Modeling*. Elsevier Inc. (2015).

Booij, H. C.; Thoone, G.: Hilbert transform in vibration analysis. *Generalization of Kramers-Kronig Transforms and Some Approximations of Relations between Viscoelastic Quantities*, 21, 1, (1982), 15–24.

Clough, R. W.; Penzien, J.: *Dynamics of Structures*. Mc–Graw Hill Inc., New York (USA) (1975).

Eastman, C. C.: *Product information bulletin Saflex DG Structural Interlayer*. Eastman AG (06 2015).

Elster, C.; Honerkamp, K.: Modified maximum entropy method and its application to creep data. *Macromolecules 24*, pages 310–314.

Elster, C.; Honerkamp, K.; Weese, J.: Using regularization methods for the determination of relaxation and retardation spectra of polymeric liquids. *Rheologica Acta 31*, pages 161–174.

Emri, I.; Tschoegl, N. W.: Generating line spectra from experimental responses. part iv: Application to experimental data. *Rheologica Acta 3*, pages 60–70.

Emri, I.; Tschoegl, N. W.: Determination of mechanical spectra from experimental responses. *International Journal of Solids and Structures 32*, pages 817–826.

Feldman, M.: Hilbert transform in vibration analysis. *Mechanical Systems and Signal Processing*, 25, 3, (2011), 735–802.

Flügge, W.: *Viscoelasticity*. Springer, Berlin (1975).

Foellinger, O.: *Laplace-, Fourier- und z-Transformation* -. VDE-Verlag, Berlin, 10. vollständ. Überarb. edn. (2011).

Hahn, S. L.: *Hilbert Transforms in Signal Processing* -. Artech House, Norwood (1996).

Honerkamp, K.: Illposed problems in rheology. *Rheologica Acta 28*, pages 363–371.

Honerkamp, K.; Weese, J.: Determination of the relaxation spectrum by a regularization method. *Macromolecules 22*, pages 4372–4377.

Kraus, M.; Niederwald, M.; Siebert, G.; Keuser, M.: Rheological modelling of linear viscoelastic materials for strengthening in bridge engineering. In: *Proceedings of the 11^{th} German Japanese Bridge Symposium*, Osaka, Japan (2016).

Kuntsche, J. K.: *Mechanisches Verhalten von Verbundglas unter zeitabhängiger Belastung und Explosionsbeanspruchung*. Springer Vieweg, Berlin (2015).

Lawson, C. L.; Hanson, R. J.: *Solving Least Squares Problems*. Prentice–Hall (1974).

Mead, D. W.: Numerical interconversion of linear viscoelastic material functions. *Journal of Rheology 38*, pages 1769–1795.

Menard, K. P.: *Dynamic Mechanical Analysis – A Practical Introduction*. CRC Press LLC, Boca Raton (USA), first edition edn. (1999).

Orbey, N.; Dealy, J. M.: Determination of the relaxation spectrum from oscillatory shear data. *Journal of Rheology 35*, pages 1035–1049.

Roylance, D.: *Engineering Viscoelasticity*. Departement of Materials Science and Engineering, Massachusetts Institute of Technology, Cambridge (USA) (2001).

Schwarzl, F. R.: *Polymermechanik*. Springer, Berlin (1990).

Tschoegl, N. W.: *The Phenomenological Theory of Linear Viscoelastic Behavior*. Springer, Berlin (1989).

Tschoegl, N. W.; Emri, I.: Generating line spectra from experimental responses. part ii: Storage and loss functions. *Rheologica Acta 32*, pages 322–327.

Address: Michael Anton Kraus, M.Sc.(hons), M.Sc., Michael Niederwald, M.Eng., University of German Armed Forces Munich, Institute and Laboratory for Structural Engineering, Werner-Heisenberg-Weg 39, 85577 Neubiberg, Germany
email: m.kraus@unibw.de, michael.niederwald@unibw.de